

Stable ferromagnetism in *p*-type carbon-doped ZnO nanoneedles

T. S. Heng,¹ S. P. Lau,^{2,a)} C. S. Wei,² L. Wang,³ B. C. Zhao,³ M. Tanemura,⁴ and Y. Akaike⁴

¹*School of Electrical and Electronic Engineering, Nanyang Technological University, Singapore 639798, Singapore*

²*Department of Applied Physics, The Hong Kong Polytechnic University, Hung Hom, Kowloon, Hong Kong*

³*Division of Physics and Applied Physics, School of Physical and Mathematical Science, Nanyang Technological University, Singapore 637371, Singapore*

⁴*Graduate School of Engineering, Nagoya Institute of Technology, Gokiso-cho, Showa-ku, Nagoya 466-8555, Japan*

(Received 20 August 2009; accepted 7 September 2009; published online 28 September 2009)

The authors report the synthesis and magnetic properties of carbon-doped ZnO (ZnO:C) nanoneedles. A saturated magnetic moment of 2.16 emu/cm³ was found in the ZnO:C nanoneedles. The samples showed anomalous Hall effect and *p*-type conduction with a hole concentration of 1.8×10^{18} cm⁻³. The ferromagnetism in the ZnO:C nanoneedles could be attributed to C substitution on the O site which introduces hole, so the *p*-*p* interaction leads to the strong spin interaction between the C atoms and carriers. It was found that the ferromagnetism and *p*-type conduction in the ZnO:C nanoneedles were stable in ambient air over a period of 1 year and annealing temperature of up to 100 °C. © 2009 American Institute of Physics.

[doi:[10.1063/1.3238289](https://doi.org/10.1063/1.3238289)]

Room-temperature (RT) ferromagnetism has been observed in a wide range of oxide materials, which do not contain ions with partially filled *d* or *f* bands. The term “*d*⁰ ferromagnetism” is given to this type of materials.¹ The examples of *d*⁰ ferromagnets include HfO₂,^{1,2} In₂O₃,^{2,3} TiO₂,² ZnO (Ref. 4) and carbon-doped ZnO (ZnO:C).^{5,6} Among these *d*⁰ oxides, ZnO:C has received significant attention because of its potential application in spintronics. Peng *et al.*⁷ showed that direct hole doping at the anion site, such as C substitution on the O site, was more effective for localizing the hole and sustaining the magnetic moment. Indeed, *p*-type conduction and anomalous Hall effect have been observed experimentally in ZnO:C thin films.⁶ Peng *et al.*⁷ also predicted that quantum confinement effect could reduce the critical hole concentration to induce ferromagnetism in ZnO nanostructures. However, it has been proved challenging to incorporate C into ZnO nanostructures effectively by conventional methods. Although graphite powder is often mixed with ZnO powder as source materials to produce ZnO nanostructures in a vapor phase process, graphite is only acted as a reducing agent for ZnO.⁸ The ZnO nanostructures are always free of C incorporation. Here we report the ferromagnetic *p*-type ZnO:C nanoneedles prepared by a low-energy (~500 eV) ion beam technique. The magnetic and transport properties of the ZnO:C nanoneedles are stable with aging time which is different from most of the transition-metal-doped ZnO (ZnO:TM).^{9,10} Furthermore, by means of anomalous Hall effect, the intrinsic ferromagnetism in ZnO:C nanoneedles is probed.

A highly texture (002) oriented starting material of ZnO films (thickness ~600 nm) was prepared on Si substrates at 300 °C by the filtered cathodic vacuum arc technique, as described elsewhere.¹¹ Prior to the fabrication of nanoneedles, a thin layer of C was deposited onto the sample in order to enhance the formation of nanostructures.¹² A C plate

serving as C source was placed perpendicular to the ZnO sample. An ion beam source with 500 eV Ar⁺ ions was irradiated simultaneously at an incidence angle of 45° to the C plate and the ZnO surface. Carbon was doped into the host material during nanoneedles formation. The undoped ZnO nanoneedles was prepared under the identical condition but without the presence of the C plate. After the fabrication of nanoneedles, the residual C layer was removed by ethanol prior to characterization. The C content of the ZnO:C nanoneedles was estimated to be ~2 at. % by the energy dispersive x-ray spectroscopy. The magnetotransport measurements were performed on a physical properties measurement system (PPMS) (Quantum Design). The standard four probe method was employed for Hall measurement. The magnetic measurements were carried out with a vibrating sample magnetometer attached to the PPMS system.

Figure 1 shows the x-ray diffraction (XRD) patterns of the ZnO and ZnO:C nanoneedles. All the peaks are well defined corresponding to a ZnO wurtzite structure. No trace of secondary phases, impurities, or graphite-related peaks can be detected within sensitivity of the XRD. The (002)

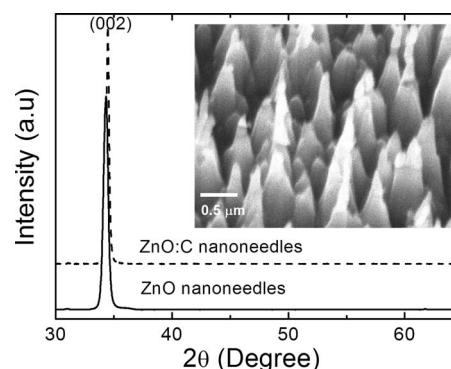


FIG. 1. Typical XRD patterns of the ZnO and ZnO:C nanoneedles. Inset is the SEM image of the ZnO:C nanoneedles array, showing the cone sharp with an average length of 250–600 nm.

^{a)}Electronic mail: apsplau@polyu.edu.hk.

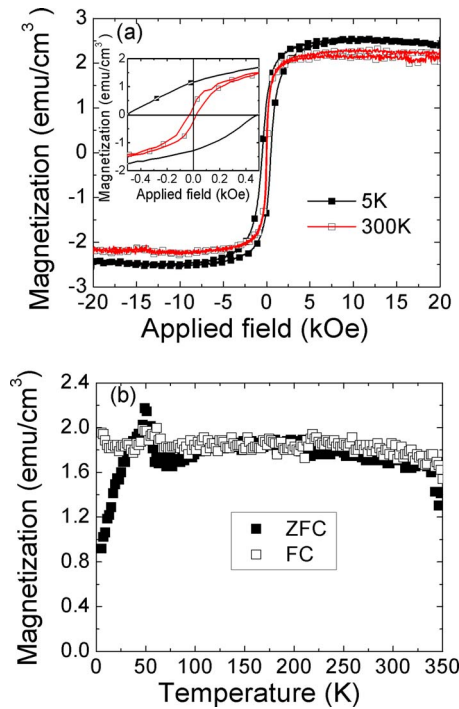


FIG. 2. (Color online) (a) Magnetic properties of the ZnO:C nanoneedles measured at 5 and 300 K. The inset shows enlarged view of hysteresis loops. (b) ZFC-FC curves of the ZnO:C nanoneedles.

peak shifts to a higher angle by 0.12° when comparing with the undoped ZnO nanoneedles. This indicates a reduction of lattice constant c with carbon doping, which is expected as smaller carbon ions is incorporated into the O sites of ZnO matrices.¹³ The surface morphology of the nanoneedles is shown in the inset of Fig. 1, possessing a needlelike structure with the length ranging from 250 to 600 nm. The diameter of the nanoneedles in the stem part is around 100 nm.

Figure 2(a) depicts the magnetic hysteresis loops of the ZnO:C nanoneedles at 5 and 300 K. The samples showed clear hysteresis loop at RT with its saturated magnetization (M_s) of 2.16 emu/cm^3 ($\sim 0.7 \mu_B/\text{C}$) as illustrated in the inset of Fig. 2(a). At 5 K, a mild increment of M_s by $\sim 17\%$ was observed. Nevertheless, a large enhancement in coercivity was detected at low temperature. The coercivity was found in the order of 30 Oe at 300 K; then it surged to ~ 490 Oe at 5 K. This broadening effect is a classical behavior of magnetic materials at low temperature. The zero-field-cooled (ZFC) and field-cooled (FC) magnetization curves in the temperature ranging from 5 to 350 K at dc field of 1 kOe are plotted in Fig. 2(b). The curves manifest ZnO:C exhibits a Curie temperature above 350 K. The ZFC-FC curves are converted into one flat curve at temperature above ~ 80 K, indicating the absence of superparamagnetism. This rule out the possibility of C clusters being the origin of the observed ferromagnetism in our ZnO:C nanoneedles. The cusp in the ZFC and FC magnetization at ~ 35 K could be attributed to spin-glass behavior.¹⁴ The spin glasslike behavior is related to the frustration originating from the coexistence of ferromagnetic and antiferromagnetic interaction. However, the ferromagnetic phase is still strongly dominant over the whole range of temperatures. It is worthwhile to highlight that no ferromagnetism can be detected in the undoped ZnO nanoneedles, implying the observed ferromagnetism is associated with the presence of C.

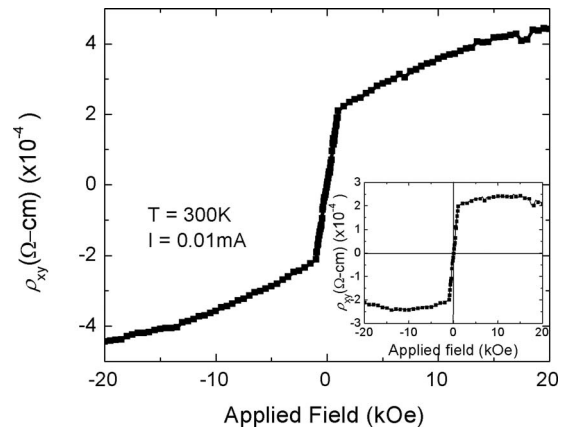


FIG. 3. The magnetic field dependence of anomalous Hall resistivity (ρ_{xy}) of the ZnO:C nanoneedles measured at 300 K. The applied magnetic field is perpendicular to the sample's plane with constant current of 0.01 mA. The ρ_{xy} data after background subtraction is displayed in the inset.

Anomalous Hall effect (AHE) is an important tool for identifying intrinsic ferromagnetic semiconductor. The Hall resistivity (ρ_{xy}) is given by sum of the ordinary Hall effect and AHE term, $\rho_{xy} = R_o B + R_s \mu_0 M$, where B , μ_0 , M , R_o , and R_s is magnetic induction, magnetic permeability, magnetization, ordinary Hall coefficient and anomalous Hall coefficient, respectively. Figure 3 shows the magnetic-field (H) dependence Hall resistivity (ρ_{xy}) of the ZnO:C nanoneedles. The field was applied perpendicular to the sample's surface at RT. At low magnetic fields (< 1 kOe), ρ_{xy} has largely linear field dependence and the anomalous contribution dominates. Above 1 kOe, ρ_{xy} increases gradually and becomes much less field dependent, which is dominated by ordinary Hall resistance. The positive slope at high field regime implies the charge carriers in the ZnO:C nanoneedles is p -type with its hole concentration of $\sim 1.8 \times 10^{18} \text{ cm}^{-3}$. It should be noted that n -type conduction was observed in the undoped ZnO films. Thus, the observed p -type conduction in the ZnO:C nanoneedles must be associated with the C doping. The experimental result is in good agreement with theoretical studies. If C substitutes O in the ZnO, the C $2p$ orbital is localized and each site creates two holes.^{5,7} The p - p interaction can lead to the strong spin interaction between the C atoms and carriers which can sustain the magnetic moment. In addition, by subtracting the linear normal Hall effect term yields a clear signature that corresponding to the AHE as shown in the inset of Fig. 3. Notably, the shape of the ρ_{xy} curve is well coincidence with the RT M - H curve as shown in Fig. 2(a), confirming intrinsic ferromagnetism in the ZnO:C nanoneedles.

It is known that ferromagnetism in ZnO:TM films or nanoparticles are not stable and will degrade with time. The degradation could take place within hour to several months after the samples were synthesized.^{2,9,10,15} Thus, it would be of interest to study the stability of the ZnO:C nanoneedles. The ZnO:C samples were kept in a transparent sample box in ambient air for a long period of time. The time dependence M_s was measured in an interval of 3 months as plotted in Fig. 4. The M_s of the ZnO:C remains constant at $\sim 2.16 \text{ emu/cm}^3$ over a period of 1 year. Our observation is stark contrast to many ZnO:TM materials where the ferromagnetism will degrade with time.^{9,10,15} It should also be noted that the hole concentration of the ZnO:C nanoneedles

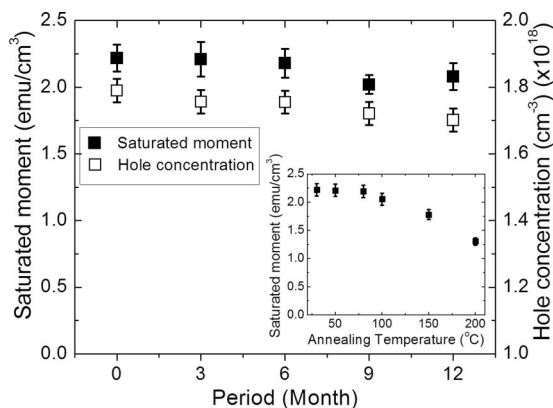


FIG. 4. The saturated magnetic moment (M_s) and hole concentration of the ZnO:C nanoneedles as a function of storage time. The inset shows the M_s dependence of the ZnO:C nanoneedles as a function of annealing temperature.

remains almost constant for the entire storage period as shown in Fig. 4, suggesting the stable p -type behavior in the ZnO:C system. The transient p -type behavior observed in most of the p -type ZnO can be attributed to either the addition of free electrons due to hydrogen or the creation of compensating defects.⁹ The conduction in ZnO:C nanoneedles does not seem to be sensitive to ambient air or oxidation process. To have better understanding of its ferromagnetic stability, a series of ZnO:C nanoneedles were annealed in air for 1 h at various temperatures ranging from RT to 200 °C. The M_s of the ZnO:C nanoneedles remains constant for annealing temperature up to 100 °C as shown in the inset of Fig. 4. Nevertheless, the M_s reduced by $\sim 40\%$ to 1.3 emu/cm³ after the sample was annealed at 200 °C. The sample annealed at 200 °C showed high resistivity and no reliable Hall measurement could be obtained. The loss of electronically active acceptor states could be explained by the generation of compensating defects such as oxygen vacancies.⁹ The ferromagnetism in the ZnO:C nanoneedles is associated with the hole and the hole could enhance the ferromagnetism, which is in good agreement with the theoret-

cal studies.^{5,7} Further experiments are needed to clarify the relationship between p -type conduction and ferromagnetism in ZnO:C nanostructures.

In summary, the origin of ferromagnetism in the ZnO:C nanoneedles can be attributed to C doping. The ZnO:C nanoneedles exhibited AHE with hole concentration of $1.8 \times 10^{18} \text{ cm}^{-3}$. The ferromagnetism and p -type conduction in the ZnO:C nanoneedles were found to be stable in ambient air for more than 1 year.

This work was partly supported by The Hong Kong Polytechnic University (Project No. 1-ZV95) and the Research Grants Council of Hong Kong (Project No. PolyU 5013/09P).

- ¹M. Venkatesan, C. B. Fitzgerald, and J. M. D. Coey, *Nature (London)* **430**, 630 (2004).
- ²N. H. Hong, J. Sakai, N. Poirot, and V. Brize, *Phys. Rev. B* **73**, 132404 (2006).
- ³R. P. Panguluri, P. Kharel, C. Sudakar, R. Naik, R. Suryanarayanan, V. M. Naik, A. G. Petukhov, B. Nadgorny, and G. Lawes, *Phys. Rev. B* **79**, 165208 (2009).
- ⁴S. Banerjee, M. Mandal, N. Gayathri, and M. Sardar, *Appl. Phys. Lett.* **91**, 182501 (2007).
- ⁵H. Pan, J. B. Yi, L. Shen, R. Q. Wu, J. H. Yang, J. Y. Lin, Y. P. Feng, J. Ding, L. H. Van, and J. H. Yin, *Phys. Rev. Lett.* **99**, 127201 (2007).
- ⁶T. S. Heng, S. P. Lau, L. Wang, B. C. Zhao, S. F. Yu, M. Tanemura, A. Akaike, and K. S. Teng, *Appl. Phys. Lett.* **95**, 012505 (2009).
- ⁷H. Peng, H. J. Xiang, S.-H. Wei, S.-S. Li, J.-B. Xia, and J. Li, *Phys. Rev. Lett.* **102**, 017201 (2009).
- ⁸B. D. Yao, Y. F. Chan, and N. Wang, *Appl. Phys. Lett.* **81**, 757 (2002).
- ⁹Q. Wan, *Appl. Phys. Lett.* **89**, 082515 (2006).
- ¹⁰T. S. Heng, S. P. Lau, S. F. Yu, H. Y. Yang, K. S. Teng, and J. S. Chen, *J. Phys. Condens. Matter* **19**, 356214 (2007).
- ¹¹Y. G. Wang, S. P. Lau, H. W. Lee, S. F. Yu, B. K. Tay, X. H. Zhang, K. Y. Tse, and H. H. Hng, *J. Appl. Phys.* **94**, 1597 (2003).
- ¹²M. Tanemura, J. Tanaka, K. Itoh, Y. Fujimoto, Y. Agawa, L. Miao, and S. Tanemura, *Appl. Phys. Lett.* **86**, 113107 (2005).
- ¹³R. D. Shannon, *Acta Crystallogr., Sect. A: Found. Crystallogr.* **32**, 751 (1976).
- ¹⁴C. Liu, F. Yun, and H. Morkoc, *J. Mater. Sci.: Mater. Electron.* **16**, 555 (2005).
- ¹⁵D. Pan, J. Wan, G. Xu, L. Lv, Y. Wu, H. Min, J. Liu, and G. Wang, *J. Am. Chem. Soc.* **128**, 12608 (2006).